Engineering Structures 213 (2020) 110515

Contents lists available at ScienceDirect

Engineering Structures

journal homepage: www.elsevier.com/locate/engstruct

Experimental and computational study on mechanical behaviour of carpentry corner log joints

Paweł Kłosowski, Anna Pestka, Marcin Krajewski, Izabela Lubowiecka*

Gdańsk University of Technology, Faculty of Civil and Environmental Engineering, Department of Structural Mechanics, ul. Narutowicza 11/12, 80 - 233 Gdańsk, Poland

ARTICLE INFO

Keywords:
Carpentry joints
Dovetail joint
Saddle-notch corner joint
Experiments
Finite element models
Architectural heritage
Timber structure
Validation of numerical modelling

ABSTRACT

This work concerns experimental and numerical research on carpentry joints used in historic wooden buildings in southeastern Poland and western Ukraine. These structures are mainly sacred buildings, and the types of corner log joints characteristic of this region are primarily saddle-notch and dovetail joints; thus, these two types of joints were analysed in this study.

The modelling of historic timber structures is a complex issue, so the following steps are necessary to obtain accurate solutions: verification, validation and uncertainty quantification. The first and third steps were performed in a previous study, so the current research aimed to validate the numerical models and perform simulations of carpentry joints. Herein, the authors created finite element models of two types of joints and subsequently analysed the mechanical behaviour of these joints.

Due to issues concerning model validation, the authors designed a testing stand for corner joints, which formed a part of a biaxial testing machine. The joints were subjected to horizontal loads (deformations), which may cause damage to the connection. Thus, special parts were designed for the stand, which made it possible to fix the joint and prevented eccentric forces that could possibly damage the machine during testing.

The authors presented the differences and similarities in the behaviour of both types of joints, emphasizing the corresponding advantages and disadvantages. In addition, the authors determined which type of joint was the most susceptible to damage and what elements failed first.

This paper also showed the complexity of modelling timber structures and the accuracy of the proposed numerical models for both types of joints through comparisons of the numerical and experimental results. This work primary addressed the problems in accurately reflecting material, load and boundary conditions in numerical modelling of tested carpentry corner log joints.

1. Introduction

The preservation and rehabilitation of historic buildings of a distinct heritage value requires an understanding of their mechanical performance (e.g., [1–3]). If such historic constructions are not adequately maintained, they may be subjected to ageing and biological or environmental degradation (e.g., [4]).

In the case of log buildings, it is important to understand the mechanical behaviour of carpentry corner joints since they are indispensable elements in the structural system of the building [5]. These joints ensure that the structural elements are appropriately positioned to properly transfer external loads. Corner joints also ensure the spatial rigidity of an entire structure and its capability to transfer loads after disassembly and reassembly [6]. The latter feature is crucial for renovation and conservation work [7,8]. There are examples of this type of object being transferred all over the world, such as the Wang Temple, which was built at the turn of the 12th century in Norway and then disassembled, transported to Karpacz (Poland) and reassembled in the 19th century.

The research reported in the literature mostly concerns carpentry joints comprising pieces at an angle, such as the birdsmouth joint in rafter to tie beam joints, scarf joints, dovetail joints or joints where the members are connected by their ends to achieve greater lengths (e.g., [9,10]). A multitude of numerical analyses (e.g., [11–14]), comparisons between numerical and experimental approaches have also been reported in the literature (e.g., [5,11,12,15–20]). The paper [11] has been concentrated on the numerical simulation of the double shear multiple dowel-type connection of wood including the post-failure domain. In [12] the authors performed experiments of the wooden logs taking into account different fiber orientation, variable specimen height and

* Corresponding author.
E-mail addresses: klosow@pg.edu.pl (P. Kłosowski), annmlecz@pg.edu.pl (A. Pestka), markraje@pg.edu.pl (M. Krajewski), lubow@pg.edu.pl (I. Lubowiecka).

https://doi.org/10.1016/j.engstruct.2020.110515
Received 10 October 2019; Received in revised form 10 January 2020; Accepted 9 March 2020
Available online 30 March 2020

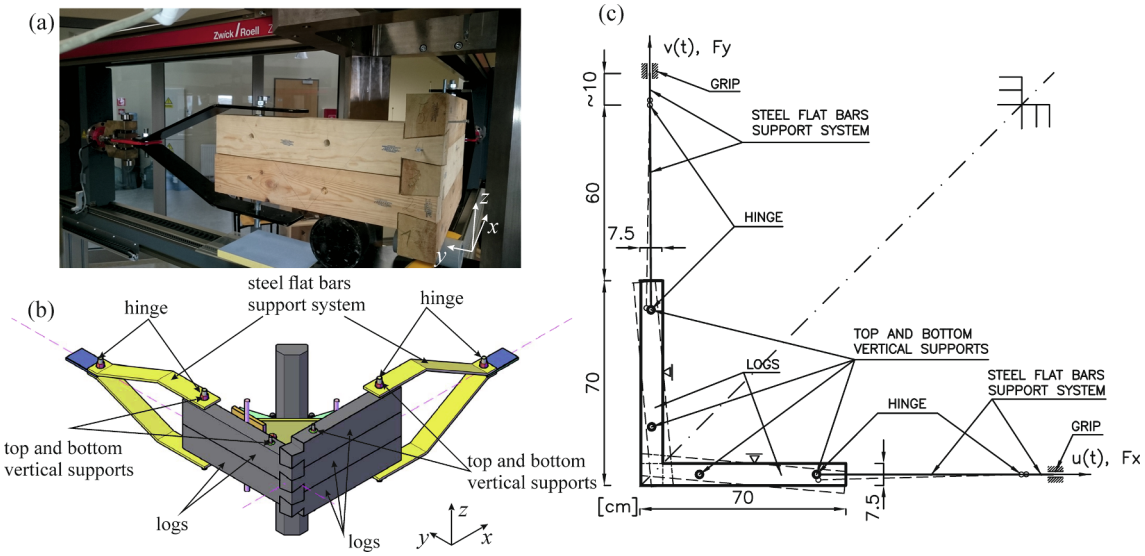

Fig. 1. Setup used to measure the forces (F_x, F_y) and displacements (u, v) of the undeformed and deformed joints during testing: (a) experimental setup for specimen with a dovetail connection, (b) view of gripping system with a tested joint specimen, (c) scheme of applied displacements.

Table 1
Material properties of wood.

Dry wood, humidity 7.2% (dovetail joint)		
Property	Units	Value
E_1 (log length direction)	N/m^2	1.195e+10
E_2 (log horizontal direction)	N/m^2	1.219e+09
E_3 (Z direction)	N/m^2	8.126e+08
ν_{12}	–	0.316
ν_{23}	–	0.469
ν_{31}	–	0.0236
Initial yield limit σ_{0k}	N/m^2	26.13e+06
Wet wood, humidity 35–40% (saddle-notch joint)		
E_1 (log length direction)	N/m^2	3.500e+09
E_2 (log horizontal direction)	N/m^2	3.570e+08
E_3 (Z direction)	N/m^2	2.380e+08
ν_{12}	–	0.316
ν_{23}	–	0.469
ν_{31}	–	0.0236
Initial yield limitσ_{0k}	N/m^2	19.18e+06

experiments of glulam beams with a circular hole. The papers [15,16] constitute a series of the research concerning the finite element model of timber-framed shear walls under quasi-static and seismic loading. In turn, the authors of the papers [17,18] presented the results of the series of experiments on structural behavior of ancient chestnut beams subjected 3-point and 4-point bending tests and determined a correlation between non-destructive tests results and mechanical wood properties obtained by destructive tests.

However, to date, few studies have been completed on carpentry connections related to corner joints of the solid walls in log-system buildings, where the logs are laid horizontally, (e.g., [5,19–21]), especially in the context of their accurate numerical modelling validated by experiments as [22] in case of full-scale experiments on log walls in seismic load; log walls with metal fasteners [23] or buckling [24]. One study [5] presented experiments and analytical models of corner log joints and walls. In their study, the authors described a stand specifically designed for testing log walls and joints. They also proposed a simplified rheological model as an assembly of spring, gap and friction pendulum elements. The model was capable of reproducing the mechanical response of log-house walls to assess timber wall behaviour, reducing the need for expensive full-scale tests.

A correct structural analysis of historic buildings can help make proper repairs and supports the solutions necessary to ensure the safety of the structure; therefore, such analyses must be based on appropriate modelling of an entire structure. This modelling approach must include an adequate choice of material properties and appropriate load and boundary conditions [25].

Numerical modelling of corner log joints is a complex issue, especially when there are planned repairs or exchanges of degraded elements. This modelling process can be performed intuitively using similar timber members; however, in recent times, new, dedicated materials (e.g., glued laminated timber, metal, carbon fibre) are more often applied in renovation and conservation (e.g., [26–30]). The difficulties with proper material modelling of log joints come from the fact that wood is a natural material (e.g., [31,32]) and that the joint geometry is complex; these joints often have imperfections that are not reflected in ideal models.

The American Society of Mechanical Engineers published the Guide for Verification and Validation in Computational Solid Mechanics, which includes guidelines that help to establish confidence in the results of complex numerical simulations [33]. Thus, the following steps towards accurate solutions are required: verification, validation and uncertainty quantification. Verification is subdivided into two major components: code verification, which involves removing programming and logic errors in the computer code, and computational verification, which involves estimating the numerical errors due to discretization approximations (e.g., convergence analysis in the finite element computations). The key tasks of the validation process are performing experiments on physical models and comparing the computational and numerical results. However, these comparisons depend on uncertainty

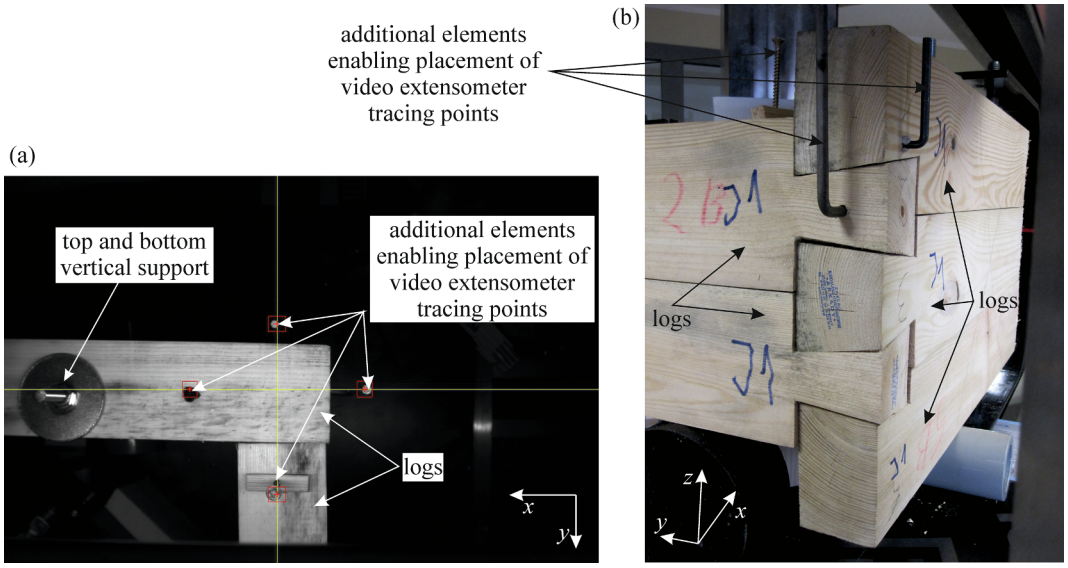

Fig. 2. Top view of a log joint during testing from the video extensometer (a), side view of connection with additional elements enabling placement of video extensometer tracing points (b).

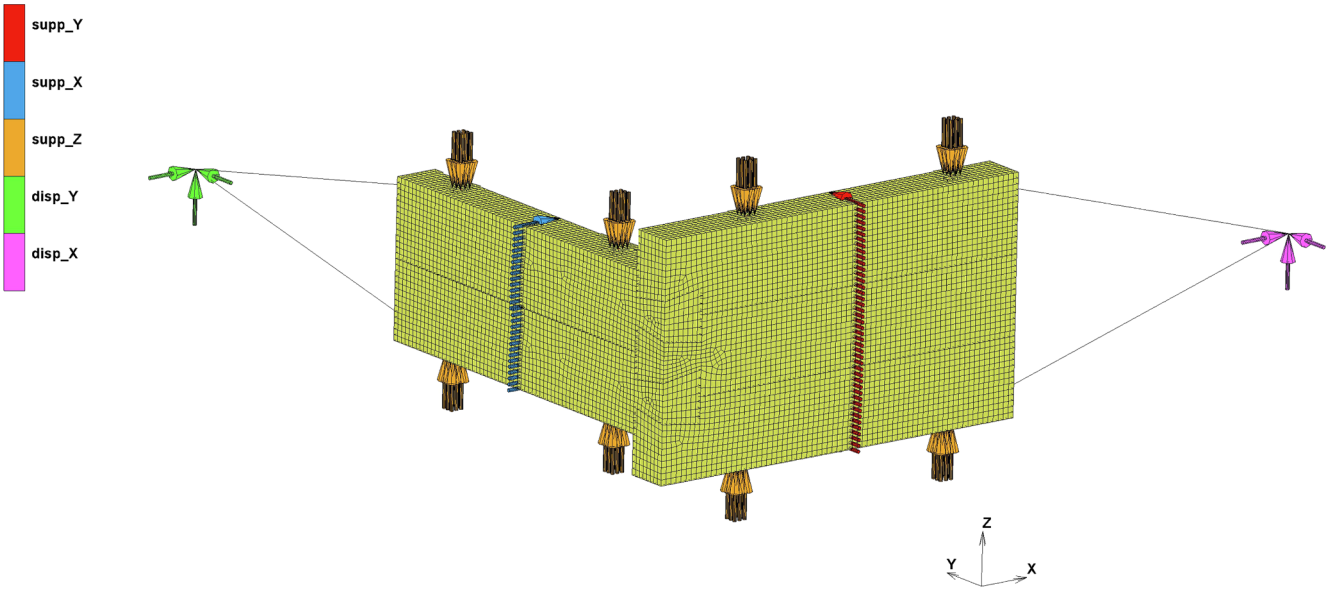

Fig. 3. Support system in a dovetail joint.

quantification and accuracy assessment of the results. Thus, uncertainty quantification is increasingly often applied as a supplementary task for structural analysis, especially in the case of natural materials, such as wood, due to the high uncertainty in mechanical characteristics [34].

Verification and uncertainty quantification were undertaken by the authors in their previous study [35]. Here, some finite element models of carpentry joints were defined and verified. Then, the impact of the material parameter variations on the mechanical performance of an entire joint was assessed by means of global sensitivity analysis. This process necessitated the subsequent uncertainty quantification. The results showed that the Young's modulus of wood in different directions was affected by structural stress variations. Thus, the material properties strongly influence the overall mechanical behaviour of the system. Some authors refer to validation discussing the mechanical performance of rounded dovetail connection [36,37] based on numerical and experimental results. They also propose probabilistic approach to predict the joint capacity and they assess the significance of geometric and material parameters of the model based on analysis of variance.

This study aimed to validate numerical models and simulations of the considered carpentry joints by means of experiments. The combination of experiments and numerical simulations provides an overview of joint performance, enabling the properties and boundary conditions to be validated at once.

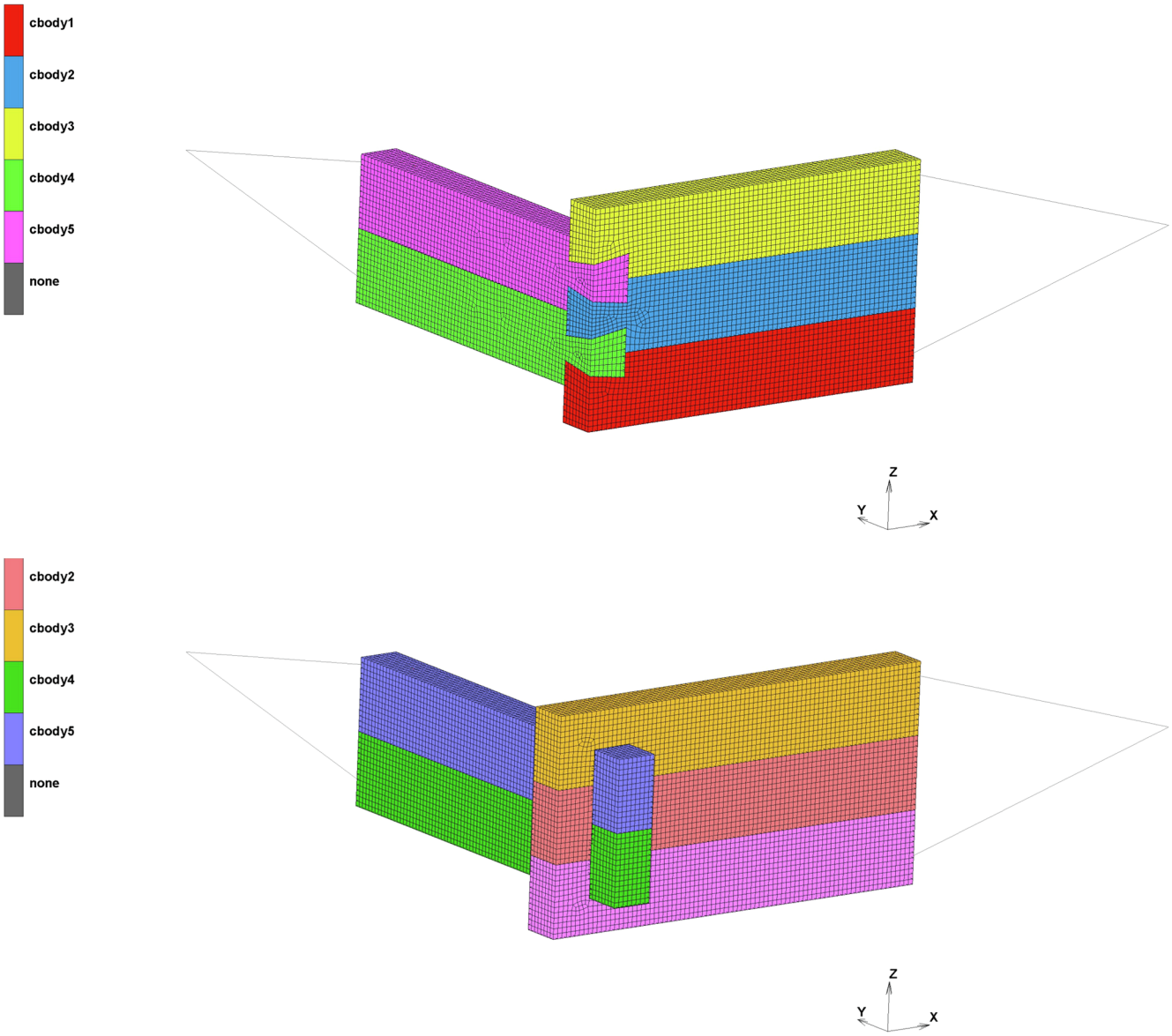

Fig. 4. Contact bodies in a dovetail and saddle – notch joint.

For the sake of the research, an experimental stand for analysing corner log joints (in a 1:2 scale) was formed by adapting a biaxial testing machine with a special type of fastening system [Patent Application number WIPO ST 10/C PL428839]. The system ensures that only axial forces are present in the testing machine grips during the experiments, which is crucial for machine safety. The advantage of the proposed setup over the alternatives described in the literature [5] is its versatility, i.e., the possibility to be applied for testing other types of corner joints.

The authors analyse the mechanical performance of carpentry joints applied in historic timber structures under horizontal deformations by means of accurate numerical models validated on the basis of experiments. Two of the most frequently used types of log joints in the walls of timber buildings in southeastern Poland and western Ukraine were selected for this research [7]: saddle-notch and dovetail joints. Apart from accurate modelling, this study investigated the most resistant joint type and the joint elements prone to damage under certain deformations, showing the differences in mechanical performance of both joint types.

A numerical model was defined, and simulations of the provided experiments were performed. Furthermore, the computational and experimental results were compared to show the modelling complexity of timber joints and to provide advice on their numerical modelling. The comparative study also indicated a need for some guidelines to properly assess the numerical results of mechanical analyses of timber structures, similar to the guidelines for the on-site assessment of timber structures defined and presented by Cruz et al. [8]. These guidelines are particularly important since repairs and conservations of historic structures are often based on finite element analysis (e.g., [3,38]).

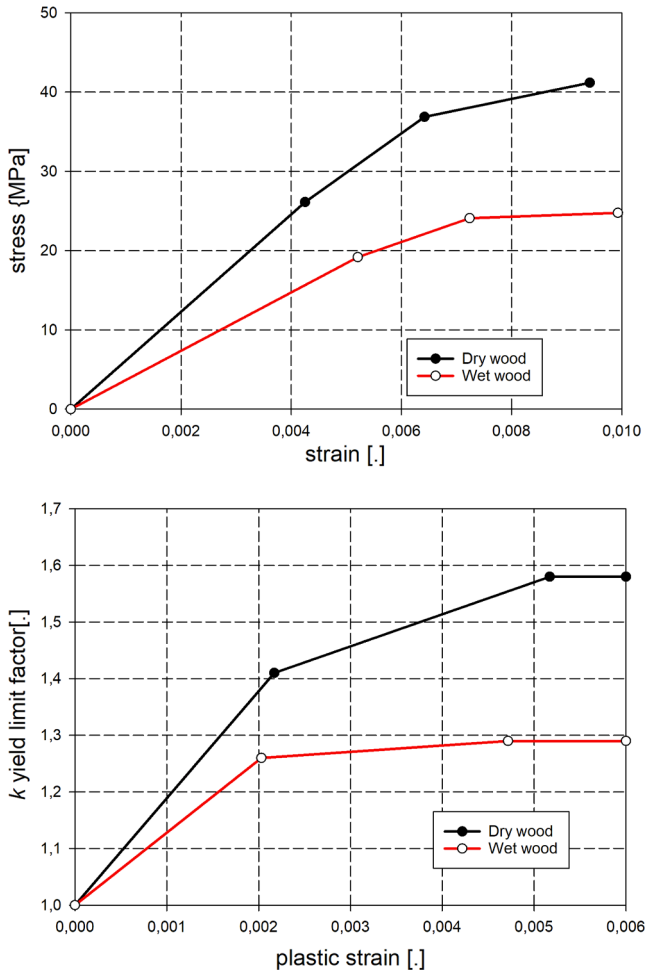

Fig. 5. Change in the elastic properties of wood.

2. Materials and methods

2.1. Experimental setup

The tests on corner connections of logs were performed on a specially adapted biaxial testing machine BIAX020. The entire set covered four machines, but only two perpendicular units were used here (Fig. 1).

The grips of the testing machine must be loaded in the direction of the machine axis. During the tests on the corner log joints, deformation of the joint caused deformation in the direction perpendicular to the axis, which may damage the testing device. To protect the grips of the machine, it was necessary to invent a special supporting system. Each arm of the tested joint was connected with the machine grip by a specially designed double-hinge system comprising steel flat bars. Therefore, the machine grip was loaded only in the direction of the machine axis. Such a supporting system turns the experimental setup into a mechanism; thus, it was necessary to introduce two additional supports (in the log midspan) perpendicular to the length of the log. These additional supports trigger deformation in the tested specimens, as shown in Fig. 1.

The tested system of logs represents a part of a wall from a real building, wherein the neighbouring logs restrict the vertical deformation of the tested logs. Therefore, in the experimental setup, the vertical deformation is limited by screws connecting all logs in each arm at the two points indicated in Fig. 1. The screws passing through all tested logs restrict vertical displacement at the place of their location. Such screws are not used in the real construction, of the historic buildings, which were the main motivation for the research. In real structures the vertical displacement is restricted by the remaining logs included in the wall.

The experimental stand was equipped with a video extensometer located above the intersection of the logs. This extensometer measured the initial phase of the deformation when the logs of two arms were nearly perpendicular to each other. The test results were recorded on a computer. Apart from the extensometer data, the set of recorded results included the experiment time (t), the current values of the grip displacement ($u(t)$, $v(t)$), and the current values of the grip forces along the test machine arm (F_x, F_y).

2.2. Specimens

Each specimen consists of five rectangular logs, and the dimensions of these logs (7.5 cm × 13.5 cm) are constructed at a 1:2 scale with respect to the dimensions of historic building logs (15 cm × 27 cm) following [39] and described in detail in [35]. The dimensions are scaled due to the size of the testing machine. The ratio of cross-section dimensions 13.5/7.5 = 1.8, which is within the range suggested in [24]. The length of the working part of the log during the test is 70 cm. The corner joint is formed from three logs in one direction (X) and two logs in another direction (Y) oriented perpendicular to the first. The logs were cut from the pine wood, whose mechanical properties have been tested in a separate part of the research (see [40]) and presented in Table 1. In [40] the 4-point bending tests on pine wood have been presented and material parameters have been determined in accordance with EN 408:2010 + A1:2012: E [41]. All tests have been performed in room temperature. In the present research the material parameters have been evaluated on the basis of compression tests. The values of the obtained material parameters are quite similar in case of 4-piont bending tests and compression tests, and also some of them are consistent with those reported in [21].

The humidity of dry wood was assessed as 7.2%; wet wood as 35–40%. Two types of log connections were formed: dovetail (without a remainder) and saddle-notch (with a 7.5 cm remainder). Two vertical holes with a diameter of 22 mm were drilled in each arm of the joint. Two bars with diameters of 20 mm were inserted (with nuts and washers preventing vertical displacements of the logs) in the holes closer to the support. These round bars together with specially formed flat steel bars also form a hinged connection between the logs and the supporting system (see Fig. 1). The 10 mm diameter bars were inserted into the holes closer to the joint point, and the logs were kept together by a special system of washers and nuts. Due to the different kinds of joints three sets of experimental connections were tested.

2.3. Test execution

The tests were performed under a constant grip constant displacement rate. In the preloading phase (up to a reaction force of 50 N), a displacement rate of 10 mm/min was applied. During the main part of the experiment, a displacement rate of 20 mm/min was applied (at both arms of a log joint). The control points of the video extensometer were

Fig. 6. A dovetail connection before and after the test.

Fig. 7. A saddle-notch connection before and after the test.

marked on two neighbouring top logs to follow the displacements between the points (Fig. 2). The use of a video extensometer requires marking on the specimen two pair of points, the displacement between which will be tracked during the test. Each pair of points lying on one video extensometer axis must be associated with a log from a different family. In addition, these points must be on the same surface. Therefore, additional auxiliary elements have been attached to the tested logs, enabling the placement of video extensometer tracking points that meet the following condition. Relevant extensometer results could be obtained when the marking point stays on the perpendicular main axis of the biaxial machine (thin cross lines in Fig. 2). During large deformations, the angle between log arms varied. Then, the markers moved along the main axis, and error was introduced into the extensometer results; therefore, these results were neglected in the evaluation.

The grip values mentioned in Section 2.1 were recorded during the

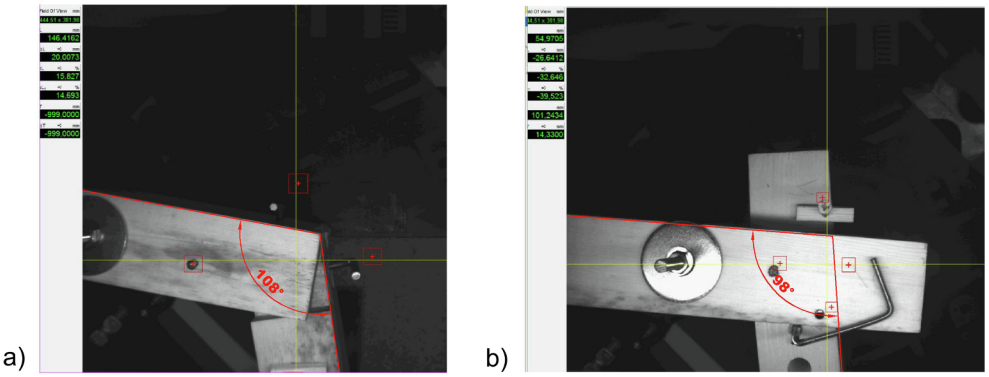

Fig. 8. Top view on deformed joints: (a) dovetail joint and (b) saddle-notch joint.

Table 2
Support displacements and reaction forces at the end of the test.

Test number	Maximum X displacement [cm]	Maximum X reaction force [N]	Maximum Y displacement [cm]	Maximum Y reaction force [N]
Dovetail connection				
1	5.00	3250	5.00	2890
2	5.90	7350	5.90	7780
3	5.40	5140	5.40	5390
4	4.30	5100	4.30	5130
5	5.40	7915	5.40	8050
6	5.70	8600	5.70	9150
Saddle – notch connection				
1	3.20	10,000	3.20	11,100
2	2.70	12,000	2.70	12,600
3	2.00	10,300	2.00	11,000
4	1.50	9500	1.50	8700
5	2.70	13,300	2.70	12,500

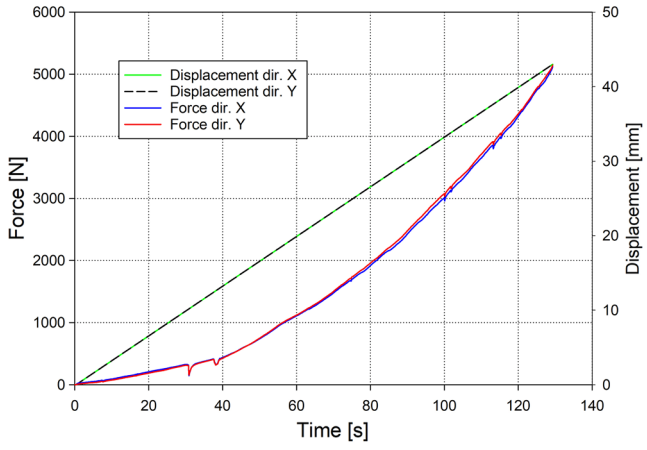

Fig. 9. Dovetail joint test No. 4: time functions of grip displacements and forces.

test. The extensometer and grip results were registered every 0.02 s or when the change in the grip force exceeded 1 N. For each test, a file was created containing over ten thousand sets of recorded values. The experiments were continued until the grip force of any arm decreased (indicating that the load-bearing capacity of the joint was reached) or when the deformation of the joint made the supporting structure touch the joint (sudden increase in force).

2.4. Finite element simulations

Models of the logs were created in Autodesk AutoCAD software. These models were meshed with eight-node hexahedron volume elements in MSC Apex and then imported (in Nastran data format) into MSC Marc/Mentat commercial finite element software. The formation of the remaining elements of each model, such as the supports and linking bars, the setting of the corresponding material properties, and the numerical computations of the tested joints were performed with MSC Marc/Mentat commercial software.

The finite element model consists of five solids of nominal dimensions (in a 1:2 scale) of each type of joint. The computations were performed in two variants. In the first variant, it was assumed that the cuts of each log were precise; thus, there were no gaps in the connections. In the second variant, to represent the natural imperfections in fitting the logs in joints, gaps of 1 mm were introduced between the log joint surfaces (not present between the logs) (see e.g., [21]).

Each log is divided into about 8000 eight-node hexahedral volumetric elements. The steel flat bars are modelled as truss elements.

The system of supports (Fig. 3) was created to express the experimental boundary conditions with the highest intended precision. Additional supports in Z direction represent round bars connecting the experimental log arms. In the location of these supports the additional link of nodes on the logs surfaces was created.

The surface-to-surface contact was applied. However a different approaches are considered in literature (see e.g., [21]), a zero coefficient of friction was assumed here, thus allowing free sliding. Normal pressure equals zero if separation occurs. Thus gaps can form in the model between bodies depending on the loading. This solution is nonlinear because the area of contact may change as the load is applied. The contact bodies of the model are presented in Fig. 4.

The material properties used in the anisotropic (see e.g., [6]) elastic-plastic model of wood were partially implemented from the author's previous laboratory tests [40] and partially based on the literature data for pine wood [42]. The assumed values are given in Table 1. Due to the observed humidity in the logs used in the experiments with the saddle-notch joint, the elastic material parameters of wet wood were applied in the simulations of the joint behaviour. In the case of the dovetail joint, which was dry, the material parameters of dry wood were applied in the computational model. Following the study presented in [38] the

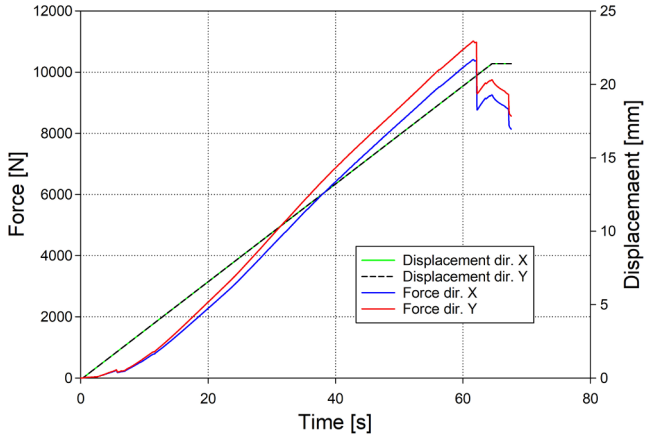

Fig. 10. Saddle-notch joint test No. 3: time functions of grip displacements and forces.

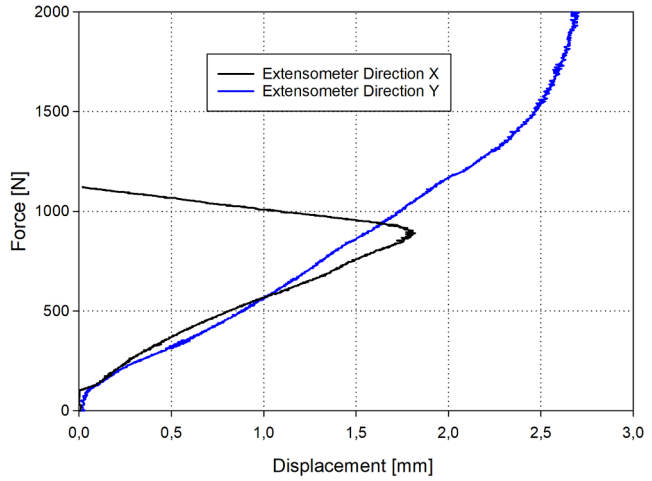

Fig. 11. Extensometer results for a dovetail joint during test No. 2.

computations employed the elastic-plastic constitutive model with hardening, and the assumed change in elastic parameters is presented in Fig. 5. This process did not consider damage effects and assumed no friction between logs, although this is definitely a limitation of this study. Applying Hill criterion, as suggested e.g., in [21], and analysing local damage area would certainly give more detailed description of the mechanical performance of the tested joints. Also a study of significance of friction coefficient by means of uncertainty quantification and global sensitivity analysis in this type of joints and analysis has been undertaken in [35]. The authors showed there, that the influence of uncertainty of friction coefficient on the stress state is negligible when compared to uncertainty of other material properties. On the other hand the friction coefficient for wet wood (slippery surface) is quite small so, in this analysis, the friction coefficient has been set up to zero.

The system was subjected to static displacements of the grip points. In 50 steps, the final position of the grips was subjected to a possible change of 4 cm along the X and Y directions. The calculation time of a single simulation performed on 11 threads of Intel9 was about 2 h.

3. Results and discussion

3.1. Results of experiments

Figs. 6 and 7 present the tested sets of two types of joints in the pre- and post-testing stages. In the case of the dovetail (six tests) joints, large deformations were observable after testing. In the saddle-notch joint case (five successful tests), the deformations were much smaller; however, the logs were seriously damaged. The maximum angle between two log families was measured. The dovetail joint finally deformed approximately 18–20°, whereas the deformation of the saddle-notch joint was approximately 10° smaller, as shown in Fig. 8.

Table 2 includes the final displacement of the grips and the corresponding forces of the testing machine (reaction). Despite the different numbers of logs in the X and Y directions (three logs along the X axis and two logs along the Y axis), the obtained reaction values converge. Substantially higher forces are measured in the saddle-notch joint tests than in the dovetail joint tests.

Figs. 9 and 10 show typical time functions of the grip displacements and corresponding forces. In the dovetail joint case, the stiffness of the joint measured by the reaction forces grows until the end of the successful part of the experiment. Later, due to large joint deformation, the logs touch the supporting system of the machine, and the experiment must be terminated. In the case of the saddle-notch joint at the beginning, rigid movement of logs is observed. Later, the increase in the reaction forces is almost linear up to the joint destruction when a sudden drop in the forces is observed.

In the course of a small number of tests, the displacements between log families in the region of the connections, which were recorded with the video extensometer, were properly registered. However, due to the change in the angle between the logs, the markers lost the position on two perpendicular lines and could not be properly followed by the video extensometer. This problem is presented in Fig. 11.

The displacement could be properly recorded up to a force of

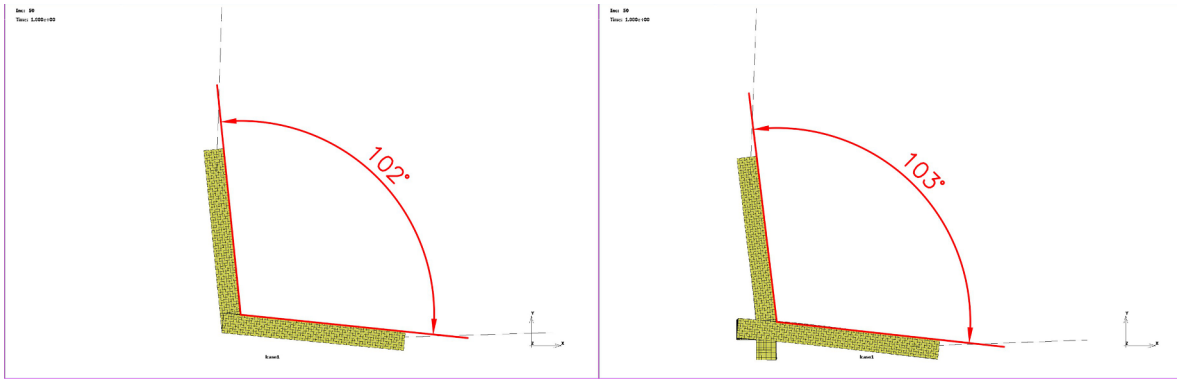

Fig. 12. Comparison of final joint deformation: (a) dovetail and (b) saddle-notch.

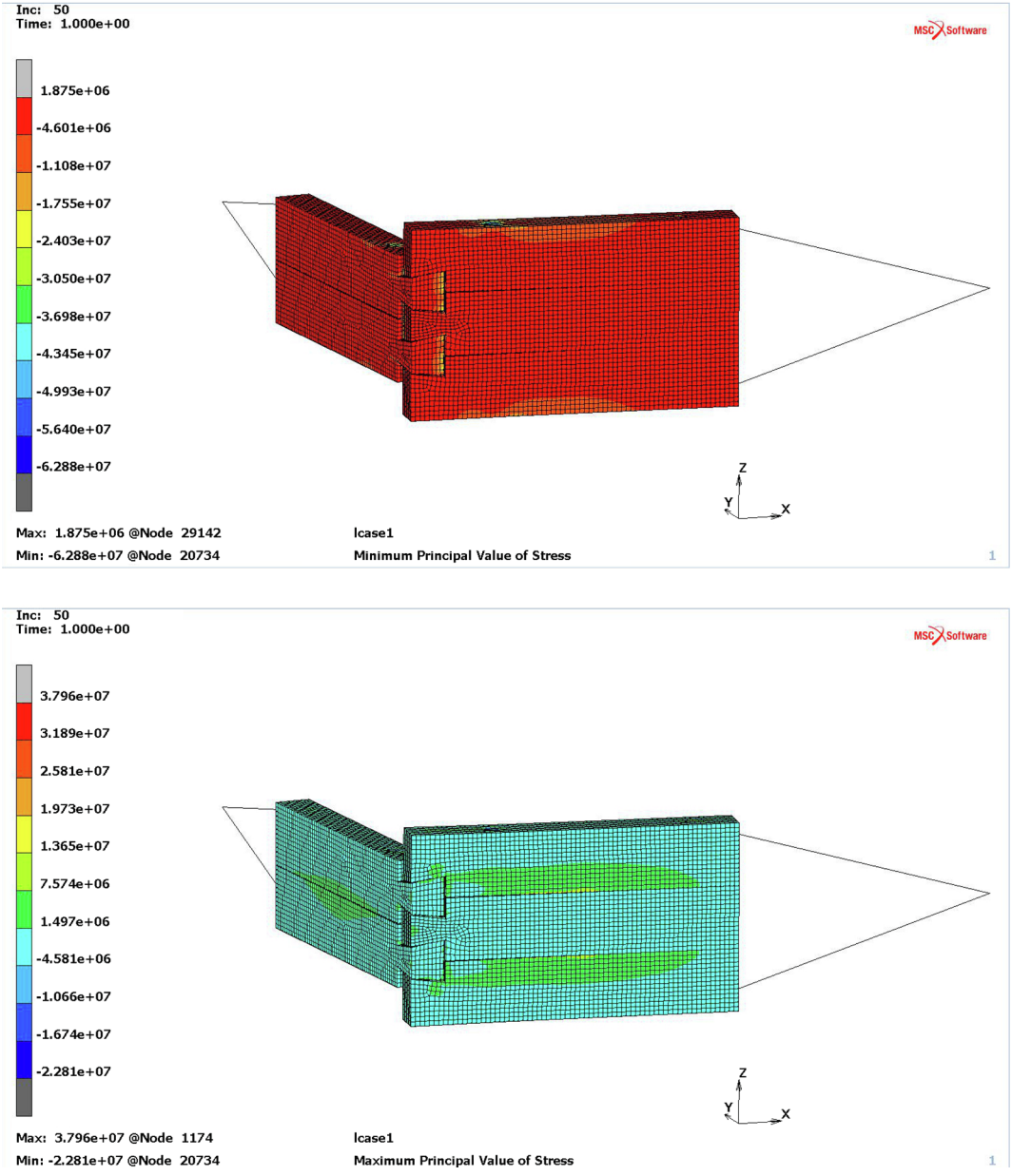

Fig. 13. Principal stress distribution in the final configuration in the dovetail joint case (outside view).

approximately 1000 N. Later, the markers in the Y direction lost their proper position. A similar situation occurred when the force in the X direction reached approximately 1500 N. The use of an image correlation technique, which is planned in future works, is bound to improve the test results.

3.2. Results of finite element analysis

The final deformation of both investigated types of joints is compared in Fig. 12. Both connections exhibit similar deformation (after full loading, the angle between log families is approximately 100°). The stress distribution in the final configuration is shown in Figs. 13 and 14. The stress distribution in the case of the 1 mm gap variant is approximately the same as that in the case without gaps. The stresses are substantially higher in the saddle-notch joint than in the dovetail joint. Fig. 15 shows structural parts that reached the yield limit (approximately 20 MPa) in the final configuration of both types of joints. In the dovetail joint case, very small pieces of logs had stresses exceeding the yield limit, whereas in the saddle-notch joint case, nearly an entire connection volume had stresses exceeding the yield limit. The principal stresses in the saddle-notch connection exceeded a typical limit stress value of pine wood (20–40 MPa) reported in the literature (e.g., [42]);

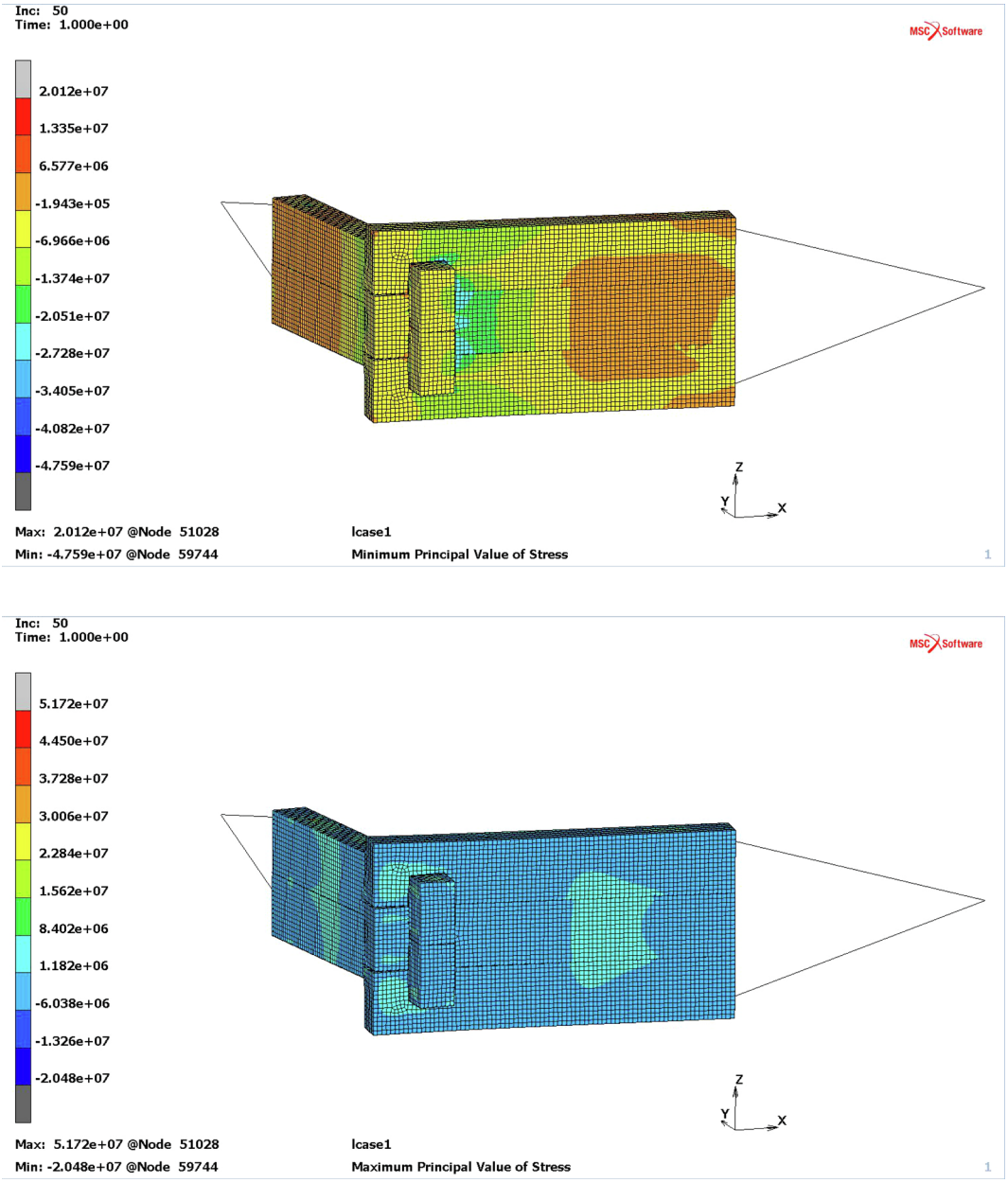

Fig. 14. Principal stress distribution in the final configuration in the saddle-notch joint case (outside view).

hence, this case is equivalent to connection damage. The stresses exceeded the limit values at 10–12 step, when the grips were displaced approximately 1 cm (see Fig. 16). This finding confirms the damage of this type of joint during an experiment (see Fig. 17).

Convergence analysis was performed by means of mesh refinement up to 740,190 linear finite elements and applying 180,325 quadratic order elements (*h* and *p* type of convergence). The difference in the obtained resultant forces did not exceed 3%, which confirms the convergence of the numerical solutions presented.

Fig. 18. Stress distribution in the saddle-notch joint case after a grip displacement of 1 cm.

4. Discussion

The study addresses the comparison of experimental and numerical results. The proposed numerical models of the saddle-notch and dovetail joints under external load are validated with experiments. The grip force-displacement functions obtained the experiments and the corresponding functions obtained from the simulations of joints with no gaps and those with 1 mm gaps are compared in Figs. 19 and 20.

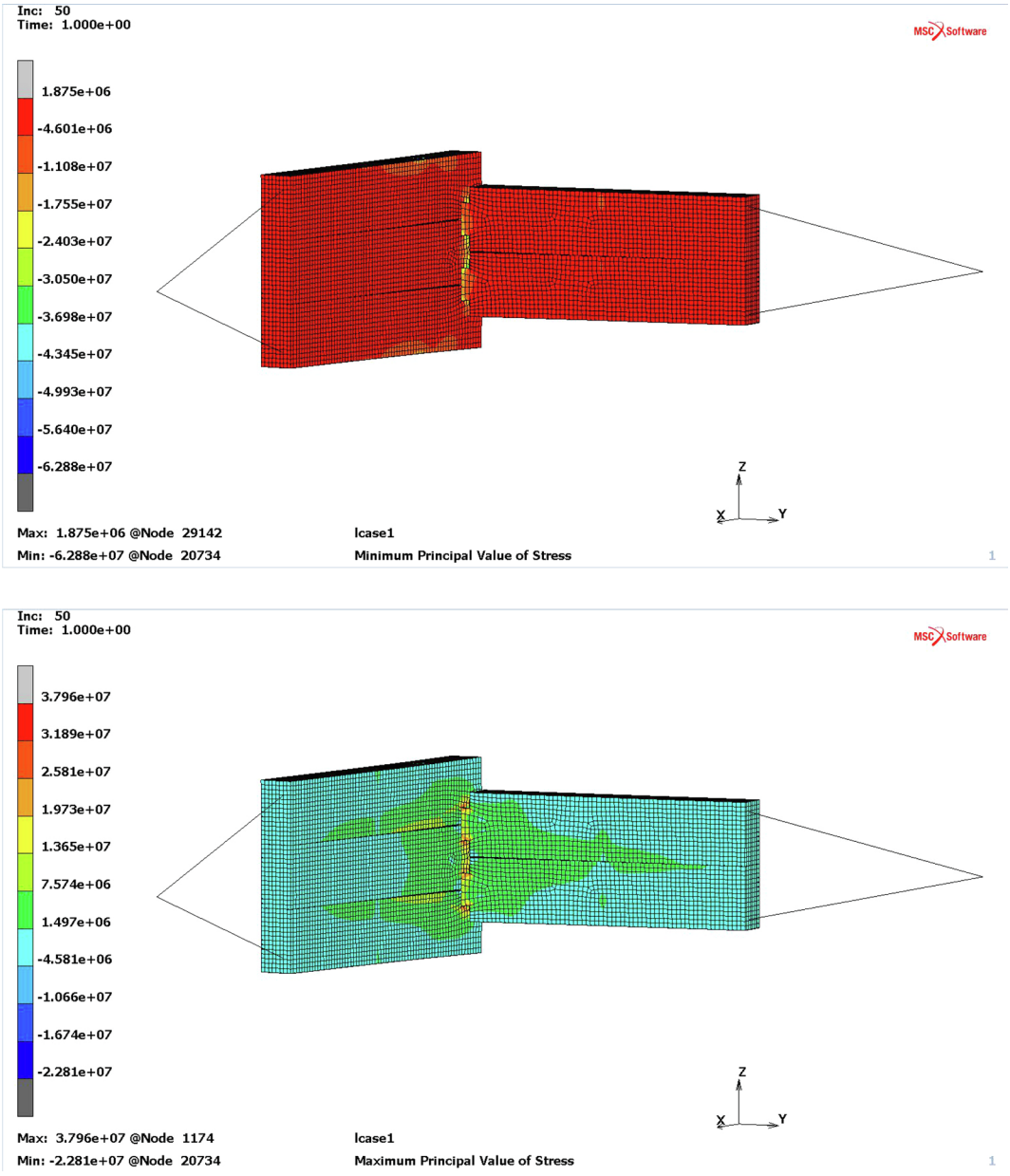

Fig. 15. Principal stress distribution in the final configuration in the dovetail joint case (inside view).

In the case of the saddle-notch joint, the experimental solution is between the no gap joint numerical solution and the 1 mm gap solution. The numerical solutions in both variants express the same joint stiffness obtained in the experiments, confirming the proper expression of geometry and material properties utilized in the numerical approach. It is difficult to assess the size of the gap between the logs in the connections. In the saddle-notch joint case, it is much easier to obtain the proper shape of the joint because the cuts must be performed in directions parallel or perpendicular to the outside surfaces of the log. Therefore, the numerical solution matches the experimental results. In the dovetail joint case, the cuts in the joint are highly complex; therefore, it is a considerable task to obtain the exact shape of the joint. Fig. 6 shows that some gaps between the logs were observed before the test. The task to create such geometry in the finite element model is much more difficult. Therefore, the characteristics of the numerical function are different from the experimental function (Fig. 19). As the gaps between the logs are gradually closing (not suddenly closing at the same time, as observed in the saddle-notch joint case), the increase in the stiffness of the joint is prolonged in time. In the numerical model where all the cut surfaces of one log are parallel to the surfaces of

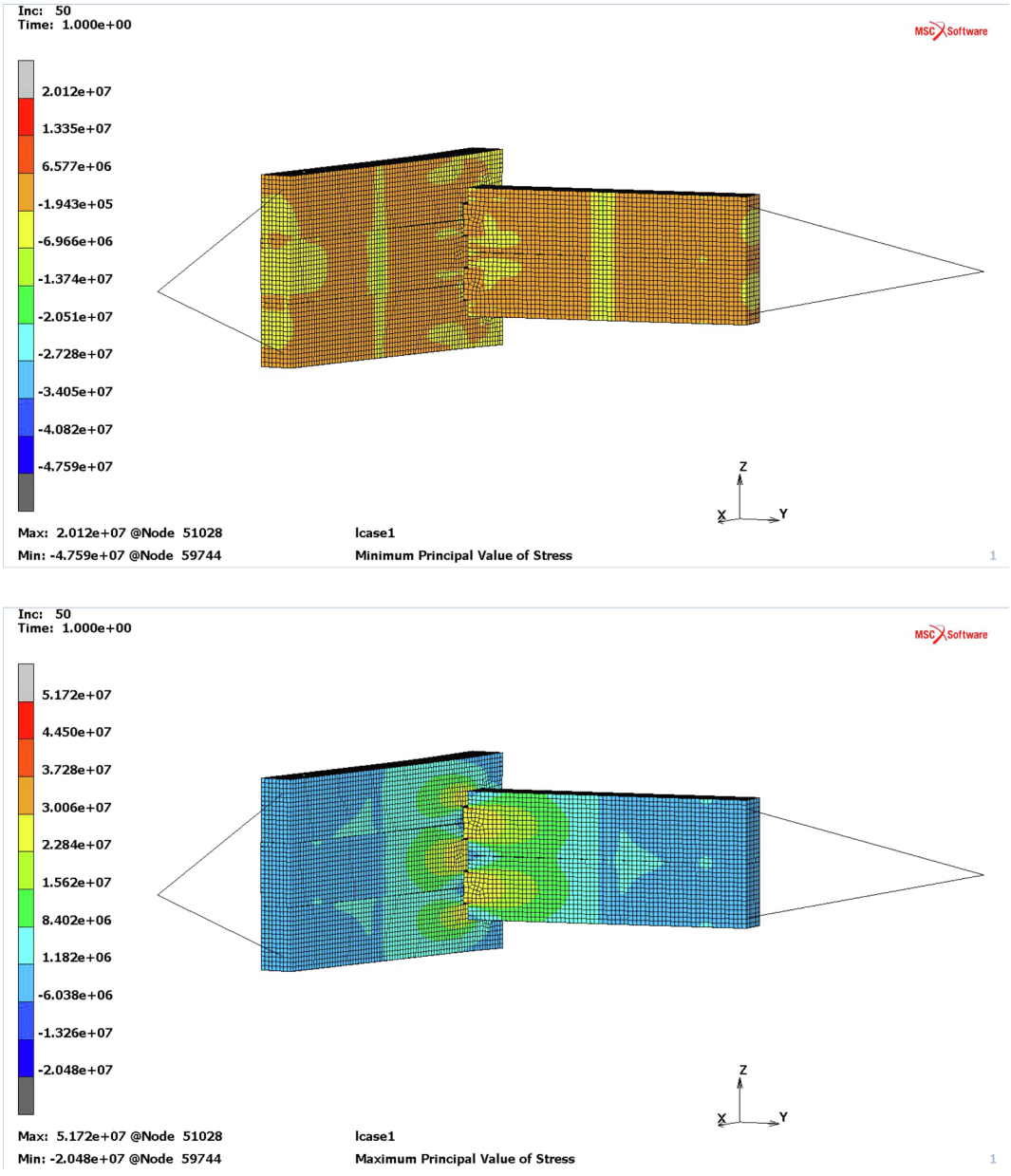

Fig. 16. Principal stress distribution in the final configuration in the saddle-notch joint case (inside view).

another log, rigid log movement is observed in the initial phase of the computations.

In summary, the dovetail connection requires a more sophisticated numerical model to represent the experimental set-up. This refined numerical model can also improve the results for the saddle-notch joint.

5. Conclusions

Analysing log corner joints is a complex problem. It is difficult to predict the joint behaviour “in situ” due to restricted access to the joints and unknown load history. Moreover, it is difficult to properly reflect the real boundary conditions in a laboratory. Log corner joints are the elements of building walls; thus, in addition to proper load and deformation, it is necessary to model the dead weight of the wall and the influence of foundations. The most difficult aspects of numerical computations are the implementation of physical properties of timber, the boundary conditions and the geometric precision of the connection. Thus, it is very important to validate the obtained computational results. Experimentation is a way the authors have chosen for the validation of computational results. Due to that reason a special testing

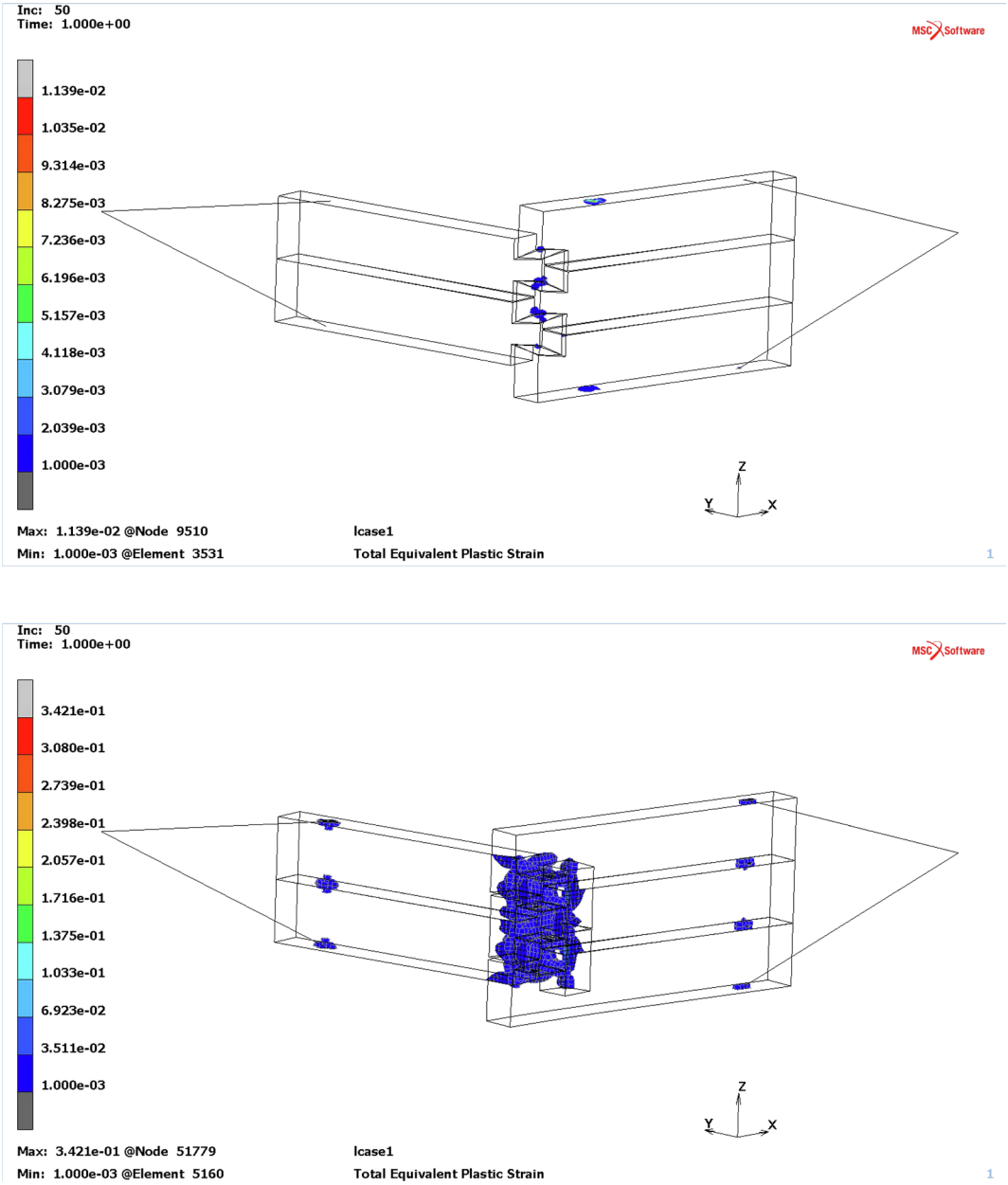

Fig. 17. Equivalent plastic strains cropped to a value of 0.001.

stand has been designed and built. Then the computational models of the joints were defined. In the current research, the authors tried to compare the mechanical behaviour of two types of joints based on the results of experimental and numerical investigations. This way the obtained numerical outcomes were assessed. The results showed that the saddle-notch joints were more rigid than the dovetail joints and that the former was more likely to be destroyed than deformed. In the numerical analysis, areas of large stress values were determined as potential areas of destruction. It was confirmed that even a large deflection in the dovetail joint does not destroy the logs; therefore, when the deformation source is removed, this joint can be easily repaired without log exchange. This aim can be difficult to achieve in the case of the saddle-notch joints. The numerical approach is a subject of permanent development that highlights damage effects. This study required sets of small-scale laboratory experiments to indicate relevant values of parameters to capture the damage effects.

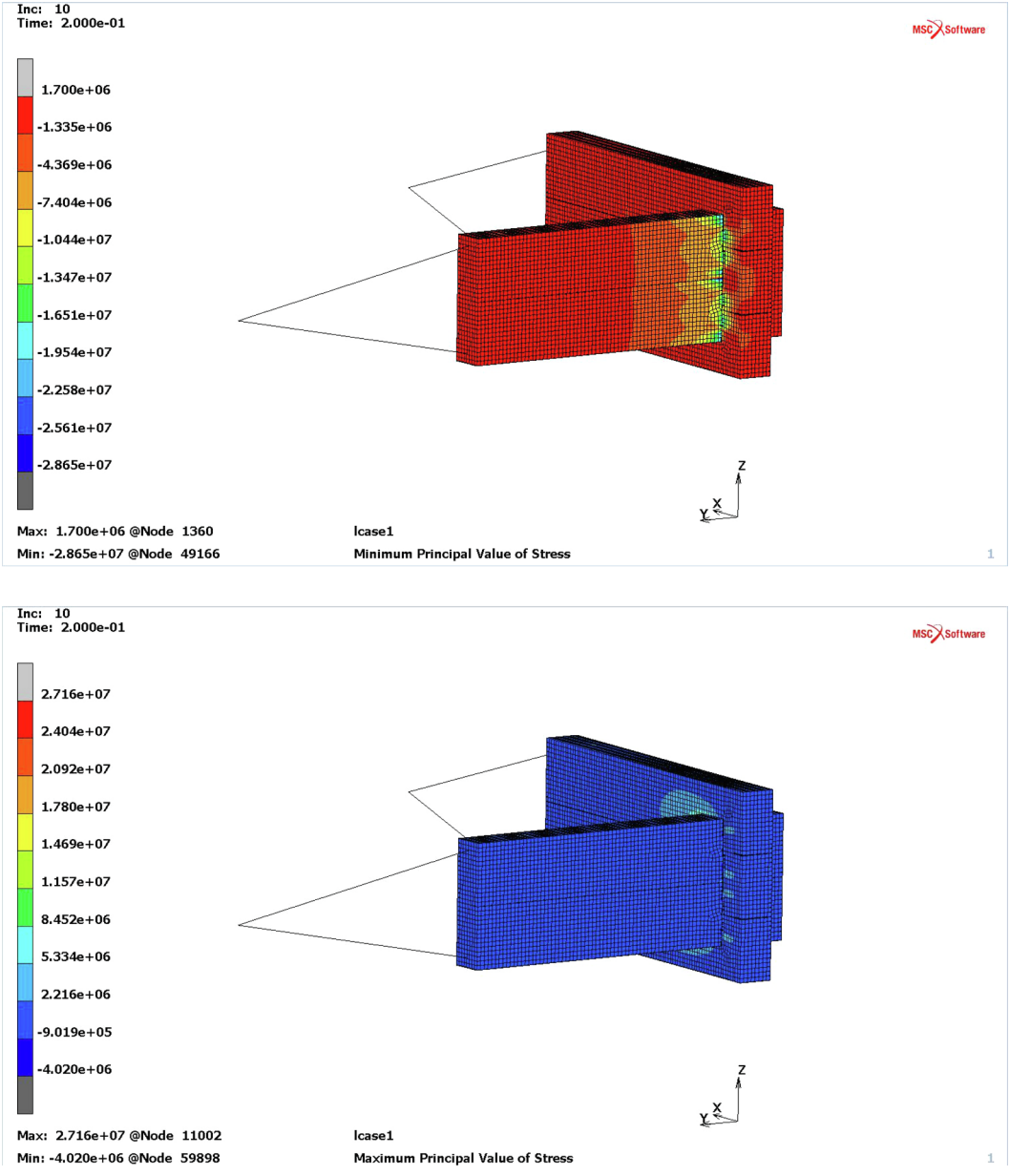

Fig. 18. Stress distribution in the saddle-notch joint case after a grip displacement of 1 cm.

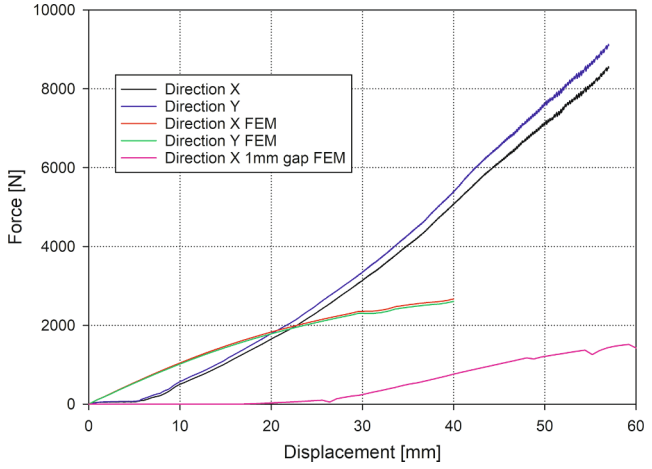

Fig. 19. Comparison of the experimental and numerical force displacement functions for the dovetail joint (test No. 6).

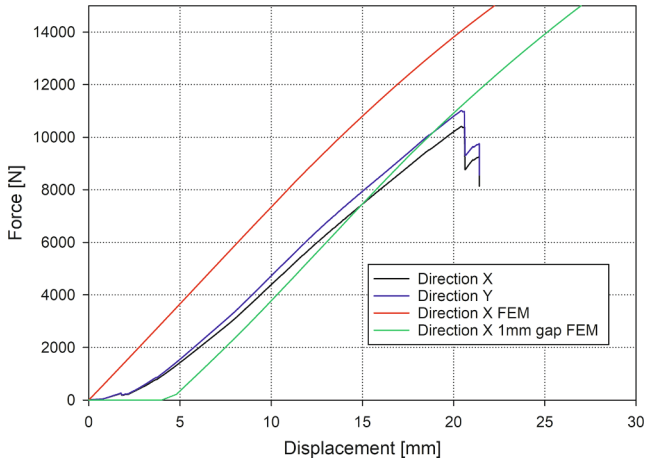

Fig. 20. Comparison of the experimental and numerical force displacement functions for the saddle-notch joint (test No.3).

CRediT authorship contribution statement

Paweł Kłosowski: Methodology, Formal analysis, Writing - original draft. **Anna Pestka:** Visualization, Investigation. **Marcin Krajewski:** Resources, Investigation, Conducting Experiments, Preparing Experimental Stand. **Izabela Lubowiecka:** Conceptualization, Investigation, Validation, Writing - original draft, Funding acquisition, Supervision.

Declaration of Competing Interest

The authors declare that they have no known competing financial interests or personal relationships that could have appeared to influence the work reported in this paper.

Acknowledgment

This work has been partially supported by the National Science Centre (Poland) [grant No. 2015/17/B/ST8/03260]. Calculations have been carried out at the Academic Computer Centre in Gdansk.

Appendix A. Supplementary material

Supplementary data to this article can be found online at https://doi.org/10.1016/j.engstruct.2020.110515.

References

[1] Armesto J, Lubowiecka I, Ordóñez C, Rial FI. FEM modeling of structures based on close range digital photogrammetry. Autom Constr 2009;18. https://doi.org/10.1016/j.autcon.2008.11.006.
[2] Lubowiecka I, Armesto J, Arias P, Lorenzo H. Historic bridge modelling using laser scanning, ground penetrating radar and finite element methods in the context of structural dynamics. Eng Struct 2009;31:2667–76. https://doi.org/10.1016/j.engstruct.2009.06.018.
[3] Bergamasco I, Gesualdo A, Iannuzzo A, Monaco M. An integrated approach to the conservation of the roofing structures in the Pompeian Domus. J Cult Herit 2018;31:141–51. https://doi.org/10.1016/j.culher.2017.12.006.
[4] Cabaleiro M, Lindenbergh R, Gard WF, Arias P, Kuilen JWG Van De. Algorithm for automatic detection and analysis of cracks in timber beams from LiDAR data. Constr Build Mater 2017;130:41–53. https://doi.org/10.1016/j.conbuildmat.2016.11.032.
[5] Grossi P, Sartori T, Giongo I, Tomasi R. Analysis of timber log-house construction system via experimental testing and analytical modelling. Constr Build Mater 2016;102:1127–44. https://doi.org/10.1016/j.conbuildmat.2015.10.067.
[6] Jasieńko J, Kardysz M. Deformation and strength criteria in assessing mechanical behaviour of joints in historic timber structures. In: Proc. 16th Int. Conf. From Mater. to Struct. – Mech. Behav. Fail. Timber Struct. ICOMOS Int. Wood Comm., 2007, p. 218–30.
[7] Jasieńko J, Nowak T, Karolak A. Historyczne z łą cza ciesielskie. (Historical carpentry joints). J Herit Conserv 2014;40:58–82.
[8] Cruz H, Yeomans D, Tsakanika E, Macchioni N, Touza M, Mannucci M, et al. Guidelines for on-site assessment of historic timber structures guidelines for on-site assessment of historic timber structures. Int J Archit Herit 2015;9:277–89. https://doi.org/10.1080/15583058.2013.774070.
[9] Aira JR, Íñiguez-González G, Guaita M, Arriaga F. Load carrying capacity of halved and tabled tenoned timber scarf joint. Mater Struct Constr 2016;49:5343–55. doi:10.1617/s11527-016-0864-y.
[10] Sangree RH, Schafer BW. Experimental and numerical analysis of a halved and tabled traditional timber scarf joint. Constr Build Mater 2009;23:615–24. https://doi.org/10.1016/j.conbuildmat.2008.01.015.
[11] Kaliske M, Resch E. Three-dimensional numerical analysis of dowel-type connections in timber engineering. Comput Struct Eng 2009:619–25.
[12] Schmidt J, Kaliske M. Models for numerical failure analysis of wooden structures. Eng Struct 2009;31:571–9. https://doi.org/10.1016/j.engstruct.2008.11.001.
[13] Khorsandnia N, Crews K. Application of Quasi-Brittle material model for analysis of timber members. Aust J Struct Eng 2015;16:99–115. https://doi.org/10.7158/S14-010.2015.16.2.
[14] Jasieńko J, Engel L, Rapp P. Study of stresses in historical carpentry joints by photoelasticity modelling. In: Lourenço, editor. Struct. Anal. Hist. Constr. Possibilities Numer. Exp. Tech., New Delhi, 6–8 November 2006: Macmillan India Ltd.; 2006.
[15] Humbert J, Boudaud C, Baroth J, Hameury S, Daudeville L. Joints and wood shear walls modelling I: Constitutive law, experimental tests and FE model under quasi-static loading. Eng Struct 2014;65:52–61. https://doi.org/10.1016/j.engstruct.2014.01.047.
[16] Boudaud C, Humbert J, Baroth J, Hameury S, Daudeville L. Joints and wood shear walls modelling II: Experimental tests and FE models under seismic loading. Eng Struct 2015;101:743–9. https://doi.org/10.1016/j.engstruct.2014.10.053.
[17] Calderoni C, De Matteis G, Giubileo C, Mazzolani FM. Flexural and shear behaviour of ancient wooden beams: experimental and theoretical evaluation. Eng Struct 2006;28:729–44. https://doi.org/10.1016/j.engstruct.2005.09.027.
[18] Calderoni C, De Matteis G, Giubileo C, Mazzolani FM. Experimental correlations between destructive and non-destructive tests on ancient timber elements. Eng Struct 2010;32:442–8. https://doi.org/10.1016/j.engstruct.2009.10.006.
[19] Branco JM, Araújo JP. Structural behaviour of log timber walls under lateral in-plane loads. Eng Struct 2012;40:371–82. https://doi.org/10.1016/j.engstruct.2012.03.004.
[20] Bedon C, Rinaldin G, Izzi M, Fragiacomo M, Amadio C. Assessment of the structural stability of Blockhaus timber log-walls under in-plane compression via full-scale buckling experiments. Constr Build Mater 2015;78:474–90. https://doi.org/10.1016/j.conbuildmat.2015.01.049.
[21] Sciomenta M, Bedon C, Fragiacomo M, Luongo A. Shear performance assessment of timber log-house walls under in-plane lateral loads via numerical and analytical modelling. Buildings 2018;8. https://doi.org/10.3390/buildings8080099.
[22] Bedon C, Fragiacomo M, Amadio C, Sadoch C. Experimental study and numerical investigation of blockhaus shear walls subjected to in-plane seismic loads. J Struct Eng 2015;141:04014118. https://doi.org/10.1061/(ASCE)ST.1943-541X.0001065.
[23] Bedon C, Rinaldin G, Fragiacomo M. Non-linear modelling of the in-plane seismic behaviour of timber Blockhaus log-walls. Eng Struct 2015;91:112–24. https://doi.org/10.1016/j.engstruct.2015.03.002.
[24] Bedon C, Fragiacomo M. Derivation of buckling design curves via FE modelling for in-plane compressed timber log-walls in accordance with the Eurocode 5. Eur J Wood Wood Prod 2017;75:449–65. https://doi.org/10.1007/s00107-016-1083-5.
[25] Palma P, Garcia H, Ferreira J, Appleton J, Cruz H. Behaviour and repair of carpentry connections – rotational behaviour of the rafter and tie beam connection in timber roof structures. J Cult Herit 2012;13:S64–73. https://doi.org/10.1016/j.culher.2012.03.002.
[26] Chang WS. Repair and reinforcement of timber columns and shear walls – a review. Constr Build Mater 2015;97:14–24. https://doi.org/10.1016/j.conbuildmat.2015.07.002.
[27] Jasieńko J, Nowak TP. Solid timber beams strengthened with steel plates – experimental studies. Constr Build Mater 2014;63:81–8. https://doi.org/10.1016/j.conbuildmat.2014.04.020.
[28] Rescalvo FJ, Valverde-Palacios I, Suarez E, Gallego A. Experimental and analytical analysis for bending load capacity of old timber beams with defects when reinforced with carbon fiber strips. Compos Struct 2018;186:29–38. https://doi.org/10.1016/j.compstruct.2017.11.078.
[29] Rapp P. Methodology and examples of revalorization of wooden structures in historic buildings. J Herit Conserv (Wiadomości Konserw 2015;43:92–108. https://doi.org/10.17425/WK43WOODENSTRUCT.
[30] Jasieńko J. Połączenia klejowe i inżynierskie w naprawie, konserwacji i wzmacnianiu zabytkowych konstrukcji drewnianych. Wrocław: Dolnośląskie Wydawnictwo Edukacyjne; 2003.
[31] Nowak TP, Jasieńko J, Hamrol-Bielecka K. In situ assessment of structural timber using the resistance drilling method – evaluation of usefulness. Constr Build Mater 2016;102:403–15. https://doi.org/10.1016/j.conbuildmat.2015.11.004.
[32] Sonderegger W, Kránitz K, Bues CT, Niemz P. Aeging effects on physical and mechanical properties of spruce, fir and oak wood. J Cult Herit 2015;16:883–9. https://doi.org/10.1016/j.culher.2015.02.002.
[33] American Society of Mechanical Engineers. Guide for verification and validation in computational solid mechanics. Am Soc Mech Eng 2006:1–15.
[34] Corradi M, Borri A, Righetti L, Speranzini E. Uncertainty analysis of FRP reinforced timber beams. Compos Part B Eng 2017;113:174–84. https://doi.org/10.1016/j.compositesb.2017.01.030.
[35] Kłosowski P, Lubowiecka I, Pestka A, Szepietowska K. Historical carpentry corner log joints—numerical analysis within stochastic framework. Eng Struct 2018;176:64–73. https://doi.org/10.1016/j.engstruct.2018.08.095.
[36] Tannert T, Lam F. Considering size effects. J Eng Mech 2010;136:358–66.
[37] Tannert T, Lam F, Vallée T. Structural performance of rounded dovetail connections: experimental and numerical investigations. Eur J Wood Wood Prod 2011;69:471–82. https://doi.org/10.1007/s00107-010-0459-1.
[38] Nowak TP, Jasieńko J, Czepizak D. Experimental tests and numerical analysis of historic bent timber elements reinforced with CFRP strips. Constr Build Mater 2013;40:197–206. https://doi.org/10.1016/j.conbuildmat.2012.09.106.
[39] Kopkowicz F. Ciesielstwo polskie. (Polish carpentry). Warsaw: Arkady; 1958.
[40] Pestka A, Kłosowski P, Lubowiecka I, Krajewski M. Influence of wood moisture on strength and elastic modulus for pine and fir wood subjected to 4-point bending tests. IOP Conf Ser Mater Sci Eng 2019;471. https://doi.org/10.1088/1757-899X/471/3/032033.
[41] EN 408:2010 + A1. Timber structures - Structural timber and glued laminated timber - Determination of some physical and mechanical properties Structures. 2015.
[42] Green DW, Winandy JE, Kretschmann DE. Wood handbook – Wood as an Engineering Material. Madison; 1999.